Structural and energetic determinants of primary proton transfer in bacteriorhodopsin†

Ana-Nicoleta Bondar,[a] Jeremy C. Smith[a] and Stefan Fischer*[b]

Received 21st November 2005, Accepted 20th March 2006
First published as an Advance Article on the web 4th April 2006
DOI: 10.1039/b516451f

In the light-driven bacteriorhodopsin proton pump, the first proton transfer step is from the retinal Schiff base to a nearby carboxylate group. The mechanism of this transfer step is highly controversial, in particular whether a direct proton jump is allowed. Here, we review the structural and energetic determinants of the direct proton transfer path computed by using a combined quantum mechanical/molecular mechanical approach. Both protein flexibility and electrostatic interactions play an important role in shaping the proton transfer energy profile. Detailed analysis of the energetics of putative transitions in the first half of the photocycle focusses on two elements that determine the likelihood that a given configuration of the active site is populated during the proton-pumping cycle. First, the rate-limiting barrier for proton transfer must be consistent with the kinetics of the photocycle. Second, the active-site configuration must be compatible with a productive overall pumping cycle.

Introduction

Bacteriorhodopsin is a seven-helical membrane protein that converts the energy of the absorbed light into a proton gradient across the membrane that is used by the cell to synthesize adenosine triphosphate.[1] The retinal chromophore is covalently attached to Lys216 *via* a protonated Schiff base.[2–4] Upon absorption of light the all-*trans* retinal isomerizes[5] to a 13-*cis* configuration[6] (Fig. 1), triggering a photocycle along which five sequential proton transfer steps result in the net transfer of one proton from the cytoplasmic to the extracellular side of the membrane.

In recent years, experiments and theory have revealed many of the details of how bacteriorhodopsin achieves vectorial proton pumping (for recent reviews, see, *e.g.*, ref. 7–11). In the ground-state bR, water-mediated hydrogen bonding interactions between

[a]*Computational Molecular Biophysics, IWR, Heidelberg University, Im Neuenheimer Feld 368, Heidelberg, Germany*
[b]*Computational Biochemistry, IWR, Heidelberg University, Im Neuenheimer Feld 368, Heidelberg, Germany. E-mail: stefan.fischer@iwr.uni-heidelberg.de*
† This paper was published as part of the special issue on Proton Transfer in Biological Systems.

Ana-Nicoleta Bondar works as a post-doctoral fellow at the University of Heidelberg, where she obtained her PhD in 2004. Her research is focussed on understanding the mechanism of conformation-coupled ion transfer in membrane proteins.

Jeremy C. Smith has held the Chair of Computational Molecular Biophysics at the University of Heidelberg since 1998. Prior to that he worked in France, England and the USA. He has authored around 200 papers on biomolecular structure and energetics.

In 1992, Stefan Fischer obtained his PhD in Biophysics from Harvard, where he continued research in theoretical biochemistry until 1995. After one year at the University of Strasbourg (France), he was Principal Scientist at Hoffmann-La Roche (Switzerland) until 1999. Since then, he is leader of the Computational Biochemistry group at the IWR of the University of Heidelberg, see http://www.iwr.uni-heidelberg.de/groups/biocomp/fischer.


Ana-Nicoleta Bondar


Jeremy C. Smith


Stefan Fischer

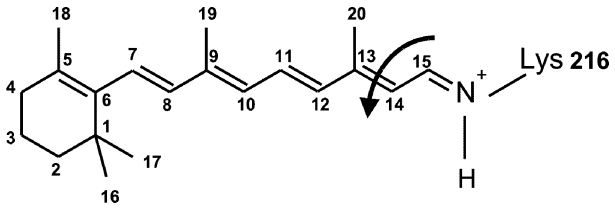

Fig. 1 Schematic representation of the retinal chromophore in the all-*trans* configuration. Upon light absorption retinal isomerizes around the C_{13}=C_{14} bond, with the formation of the 13-*cis* state.

the protonated retinal Schiff base and its complex counterion (Asp85, Asp212, Arg82, and water molecules[12–17]) stabilize the high pK_a value of the Schiff base,[7,17,18] rendering the transfer of the Schiff base proton to Asp85 energetically unfavorable.[19] In the K intermediate state, the 13-*cis* retinal chomophore is highly twisted,[20–22] the twist contributing to the initial storage of the energy of the absorbed photon.[20,21,23–25] The breaking of the hydrogen-bond-mediated connection between the Schiff base and Asp85 observed in K concurs with the previous suggestion of a light-induced separation of the Schiff base from its counterion[26–29] that leads to changes in the relative pK_a of the proton donor (the Schiff base) and acceptor (Asp85) groups.[28–30] As a result of these pK_a changes, during the L-to-M transition the retinal Schiff base proton is transferred to Asp85.[31,32]

In spite of the relatively short distance between the proton donor and acceptor groups (~4 Å), conflicting information on the structural details of the L intermediate state has led to debates over the mechanism of this primary proton transfer from the retinal Schiff base to Asp85 (see, *e.g.*, ref. 11 and 33). An orientation of the Schiff base towards Asp85 (*i.e.*, towards the extracellular side and in the direction of the net pumping) would require considerable twist around the C_{15}=N bond (Fig. 1), but would allow proton transfer *via* water w402.[34] In the case of a cytoplasmic-oriented retinal Schiff base (Fig. 2), direct[33] and *via* Thr89[33,35] proton transfer pathways were suggested. The direct proton transfer path would require local perturbations in helix C and twisting motions of the retinal chain.[7] That retinal can be quite

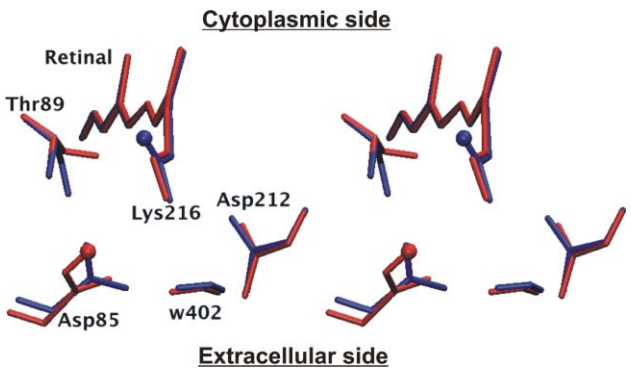

Fig. 2 Structural rearrangements triggered by the primary proton transfer. The energy-optimized pre-proton transfer state is shown in blue, overlapped with the post-transfer state, in red (stereo, crosseyed). The proton transferring from the Schiff base to Asp85 is depicted with a small sphere. In the pre-proton transfer state, the Thr89 hydroxyl group hydrogen bonds to the retinal Schiff base. The groups shown form the quantum mechanical region.

flexible has been observed in molecular dynamics simulations on bacteriorhodopsin[33,36] and rhodopsin.[37,38]

An exhaustive investigation of the pathways for primary proton transfer compatible with a productive photocycle[39,40] indicated that, within the accuracy of the computational method, three very different proton transfer mechanisms have barriers consistent with experiment.[41] Starting from a cytoplasmic orientation of the retinal Schiff base, the proton may be transferred directly to Asp85, or *via* concerted mechanisms in which Thr89 or Asp212 and water w402 act as intermediate carriers for the proton. Of these three almost isoenergetic pathways, the direct proton transfer pathway is of particular interest. The direct pathway involves a large twist of the retinal chain and flexible deformation of the surrounding protein. Thus, the flexibility and the electrostatic environment of the protein combine to shape the reaction mechanism.

In what follows we restrict ourselves to examining the energetics of the direct proton transfer mechanism as a function of the active site configuration. Furthermore, we discuss the likelihood that conformational candidates for the pre-proton transfer states are populated and lead to deprotonated retinal states capable of receiving a proton from the cytoplasmic Asp96, as required for a productive overall pumping cycle.

Computer simulations of proton transfer in bacteriorhodopsin

The details of the calculations were described elsewhere.[39,40] Briefly, the protein was partitioned into quantum mechanical (QM) and molecular mechanical (MM) regions. The QM region (depicted in Fig. 2) comprised the entire retinal molecule, the side-chains of Lys216, Asp85, Thr89 and Asp212, and water w402 (86 atoms). Hydrogen link atoms[42] were attached to C_β of Lys216 and to C_α of Asp85, Thr89, and Asp212. The quantum mechanical region was modelled with the SCC-DFTB method[43] which combines computational efficiency with accuracy in describing the retinal geometry and torsional barriers[44] and in the calculation of proton transfer barriers.[39,40,45] The pathways for proton transfer and retinal configurational changes were determined using the Conjugate Peak Refinement algorithm (CPR[46]) as implemented in the TReK module of CHARMM.[47] Starting from energy-optimized reactant and product states and an initial guess of the path (*e.g.*, an interpolation between reactant and product coordinates), CPR optimizes the structures along the path until it finds a minimum-energy pathway in which the maxima are first-order saddle points of the potential energy surface. These saddle points correspond to the transition states of the reaction, which define the reaction mechanism.

Calculations using each of five different crystal structures of the K, L, and M-state structures have indicated that the proton transfer barrier is determined mainly by the configuration of the active site (retinal isomeric state, presence of water molecules).[39] Upon geometry optimization, flexibility allows the retinal environment to adapt to the configuration and protonation state of the retinal. The protein structures used in the present proton transfer calculations were derived using the PDB entries 1QKO[48] and 1O0A[34] as starting coordinates. To simplify the calculations, and since there are no significant protein conformational changes in the first half of the photocycle,[49] the deprotonated retinal states were

derived by using same PDB entries as for the protonated states above. In the pathways for the conversion of protonated retinal from 15-*anti* to 15-*syn* the PDB entry 1M0K[20] was also used.

Unless otherwise specified, the protein surrounding the quantum mechanical region was allowed to move during the calculations. This mobile protein environment comprised the first layer of amino acids surrounding the quantum region, as well as other protein groups and water molecules that could respond structurally to the proton transfer and retinal configurational changes in the active site. The entire mobile region comprises ~830 atoms. The coordinates of the remaining protein groups and water molecules were fixed at their values from the crystal structure.

Local protein flexibility enables direct proton transfer

Due to the unfavorable relative orientation of the proton donor and acceptor groups, one would suspect that a direct proton transfer is unlikely in the case of a 13-*cis*, 15-*anti* retinal with the Schiff base pointing to the cytoplasmic side[50,51] as shown in Fig. 2. Indeed, when only the quantum mechanical groups are allowed to move, the rate-limiting barrier of the direct proton transfer was calculated to be 23.4 kcal mol^{-1} [39] ($\lambda = 0.66$, (■) in Fig. 3). This is much higher than the ~13 kcal mol^{-1} enthalpy of activation estimated from experiment.[41] The large computed barrier is due mainly to interactions within the quantum mechanical region (*i.e.*, the interaction energy of the quantum electrons and nuclei, 12.5 kcal mol^{-1}), and to non-bonded interactions between the quantum region and the remaining protein treated with classical molecular mechanics (9.1 kcal mol^{-1}). This latter energy term denotes the sum of the van der Waals interactions between the quantum and classical atoms, and the Coulombic interactions between the Mülliken charges of the quantum atoms and the partial charges of the classical atoms.[45] The computed total energy change upon proton transfer is endergonic by 10.6 kcal mol^{-1}. This endergonicity is entirely due to non-bonded interactions between the active site groups and the surrounding protein environment, because the protein is prevented from adjusting its conformation after proton transfer.[40]

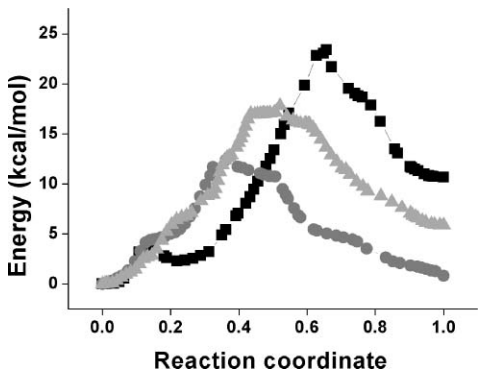

Fig. 3 Role of protein flexibility in the direct proton transfer pathway. The following regions were allowed to move in the optimization of the path structures: (■) only the quantum mechanical region (see Fig. 2) (the remaining protein is fixed); (▲) the quantum mechanical region and only protein residues Ala81 to Leu93 from helix C; (●) the whole protein environment (as described in the section 'Computer simulations of proton transfer in bacteriorhodopsin') is mobile. The reaction coordinate is the normalized sum along the path of the root-mean-squared changes in all atomic coordinates.[46] Reaction coordinate '0' corresponds to the reactant conformer (proton on the Schiff base); reaction coordinate '1' is the product conformer (proton on Asp85).

When the protein environment is treated as flexible during the reaction, the calculated barrier of direct proton transfer drops to 12.4 kcal mol^{-1} [39] ($\lambda = 0.36$, (●) in Fig. 3), *i.e.*, to a value consistent with the experiment.[41] Most of this energy barrier (8.9 kcal mol^{-1}) arises from non-bonded interactions between the quantum mechanical groups and the protein environment, which oppose proton transfer and de-stabilize the post-transfer state. Rearrangements of the retinal region in the product state, allowed by the flexible protein environment, *e.g.*, movement of the protonated Asp85 side-chain away from the deprotonated Schiff base and towards the extracellular side (Fig. 2), contribute to lowering the reaction energy, such that the neutral (product) and the ion-pair (reactant) state are almost isoenergetic.[40] In the late-M state, further conformational changes lead to a relaxation of the non-bonded interactions between the active site and the protein environment.[40] The structural changes observed here for the post-proton transfer state are consistent with previous mechanisms suggesting a separation of the Schiff base from its counterion upon canceling of the electrostatic attraction between these groups.[7,8,35,52,53]

The ability of the Asp85 side-chain to move towards the protonated Schiff base to assist proton transfer is largely influenced by hydrogen-bonding interactions with water w402. In the absence of w402, bringing Asp85 and the Schiff base to within proton transfer distance no longer involves the transient breaking of the Asp85:w402 hydrogen bond, such that the energy barrier for direct proton transfer is reduced from 12.4 kcal mol^{-1} to 6.3 kcal mol^{-1}.[39] Enhanced local flexibility of the Asp85 side-chain was also observed when computing the direct proton transfer[54] in a putative L-state structure in which only one water molecule is located in the cavity below Asp85.[55] The local flexibility of the carboxylate at position 85 can be further increased by increasing the length of its side-chain, *e.g.*, as in the Asp85Glu mutant. Consistent with experiments indicating significantly faster retinal deprotonation upon replacement of Asp85 with glutamate,[56–60] in the Asp85Glu mutant the computed rate-limiting barrier for proton transfer is 7.6 kcal mol^{-1}, *i.e.*, ~5 kcal mol^{-1} less than in the wild-type protein. Moreover, as had been discussed before,[7,60] relative to the wild-type protein the Asp85Glu mutant requires less structural rearrangements for bringing the proton donor and acceptor groups to within direct proton transfer distance. This confirms the importance of carboxylate flexibility in accelerating the direct proton transfer mechanism.

Consistent with previous suggestions,[7,39] helix C is an essential player in the flexibility-induced lowering of the rate-limiting barrier and the reaction energy. Test calculations with a mobile region consisting of, in addition to the quantum region, only of residues Ala81 to Leu 91 on helix C, Trp182, water w401 and w406, showed a decrease of the rate-limiting energy barrier ($\lambda = 0.52$, (▲) in Fig. 3) and of the reaction energy by 5.6 kcal mol^{-1} and 4.7 kcal mol^{-1} respectively, relative to the case where only the quantum region is allowed to move.

Role of specific protein groups in proton transfer

The barrier for the transfer of the Schiff base proton to Asp85 is 11–13 kcal mol^{-1} and the reaction is approximately

isoenergetic,[39,41] in spite of the fact that the intrinsic proton affinities of the isolated proton donor and acceptor groups in the gas phase would favor the protonated Asp85 state by ~100 kcal mol^{-1}.[40] A detailed analysis of the role of the active-site groups and the protein electrostatic interactions has demonstrated how the protein shapes the proton transfer energy profiles and stabilizes the proton on the retinal Schiff base.[40] In a minimal gas-phase proton transfer system consisting of retinal and Asp85, direct proton transfer is barrierless and the protonated Asp85 product state is favored by ~17 kcal mol^{-1}. When the highly-conserved Thr89 and Asp212[61] are also included in the calculations the ion-pair reactant state is significantly more stable than in the minimal system, indicating that electrostatic interactions between the ion-pair and these protein groups are key components of the mechanism by which bacteriorhodopsin controls the protonation state of the retinal chromophore. When the entire protein environment is present, the ~12 kcal mol^{-1} proton transfer barrier is due to the Coulombic and van der Waals interactions between the quantum mechanical reaction region and the classical protein environment.

Retinal states compatible with proton transfer

Vectorial pumping by bacteriorhodopsin requires that following photoisomerization and formation of the K intermediate, the highest energy barrier separating K from M is smaller than the energy barrier for the thermal *cis–trans* back isomerization. Furthermore, once deprotonated, the retinal Schiff base must be able to orient towards the cytoplasmic side of the membrane, from where it has to be reprotonated in a subsequent step of the photocycle (the proton donor is Asp96). The directionality of the early photocycle steps is achieved by controlling the retinal twist, which is finely tuned such that enough energy is stored to drive the photocycle, while maintaining the barrier for the *cis–trans* isomerization high enough to prevent thermal back isomerization.[25] By crossing over an energy barrier of ~3 kcal mol^{-1}, the twisted, extracellular-oriented K-state retinal can rapidly relax to a 13-*cis*, 15-*trans* state where the Schiff base is oriented towards the cytoplasmic side of the membrane.[39] From this configuration, deprotonation of the retinal Schiff base can occur over a barrier of ~12 kcal mol^{-1},[39,40] close to the ~13 kcal mol^{-1} enthalpy of activation for the L-to-M transition derived from experiments.[41] The deprotonated retinal Schiff base then points to the cytoplasmic side of the membrane, as required for the subsequent reprotonation step. The ensemble of these observations suggests that 13-*cis*, 15-*anti* conformations of protonated retinal with a cytoplasmic orientation of the retinal Schiff base are compatible with a productive proton pumping.

An extracellular Schiff base orientation achieved, *e.g.*, through rotation around the C_{15}=N bond leading to a twisted 13-*cis*, 15-*syn* retinal would have the appealing consequence of a favorable geometry of the proton donor and acceptor groups in the pre-transfer state. Thus, proton transfer could occur *via* water w402[11,34] with a low rate-limiting energy barrier of 7.3 kcal mol^{-1}.[40] An even lower energy barrier of 5.9 kcal mol^{-1} was found for the direct proton transfer from the 15-*syn* retinal configuration.[40] The lower barrier for the direct proton transfer in the case of an extracellular-oriented (as compared to the cytoplasmic-oriented retinal Schiff base) is consistent with the importance of specific donor/acceptor geometries in proton transfer reactions, and in particular for bacteriorhodopsin (see, *e.g.*, ref. 18, 59, 60, 62–66). However, the fact that the deprotonation of 13-*cis*, 15-*syn* retinal has a low energy barrier does not suffice to imply that this pathway is followed during the light-adapted photocycle. Indeed, the involvement in proton transfer of a particular retinal configuration depends not only on the associated rate-limiting barrier for proton transfer, but also on compatibility with the entire photocycle. That is, one must also consider the likelihood that a specific retinal state is sampled *prior* to proton transfer, and that following deprotonation it is capable of reprotonation from Asp96. The calculations suggest that these two essential requirements are not fulfilled in the case of the twisted 13-*cis*, 15-*syn* retinal. First, the barrier for a K-like 13-*cis*, 15-*anti* retinal to convert into 13-*cis*, 15-*syn* is ~19 kcal mol^{-1}, incompatible with the microsecond timescale of the K-to-L transition.[40] Second, upon deprotonation retinal remains in the 13-*cis*, 15-*syn* conformation, with the Schiff base oriented towards the extracellular side and inaccessible to reprotonation from Asp96. Reorientation of the deprotonated retinal Schiff base towards Asp96 requires an energetically unfavorable rotation around the C_{15}=N double bond: In the gas phase, the energy barrier for a 90°-torsion around C_{15}=N is ~39 kcal mol^{-1}.[67] In a flexible protein environment, our preliminary reaction pathway calculations indicate an energy barrier of ~25 kcal mol^{-1} for the extracellular-to-cytoplasmic 15-*syn* to 15-*anti* reorientation of the deprotonated retinal Schiff base. This barrier is too high to be consistent with the millisecond timescale of the whole photocycle. Thus, although the 13-*cis*, 15-*syn* retinal conformer possesses a geometry favorable for proton transfer, it is unlikely to participate in proton pumping.

Conclusions

In this review we have examined several structural and energetic determinants of the direct proton transfer mechanism in bacteriorhodopsin. Consistent with previous suggestions[7,33] the calculations reveal an essential role of the retinal twisting motions and protein flexibility in enabling the direct proton transfer from the cytoplasmic-oriented retinal Schiff base to Asp85. Elasticity of helix C is of particular importance in lowering the energy penalty to be paid in conformational strain for bringing the donor–acceptor distance to within proton transfer range. A similar role of helix C has been revealed in the homologous protein halorhodopsin, a light-driven inward chloride pump. There, the flexibility of helix C allows the transient opening of a passage for the voluminous chloride anion.[68]

For the proton-pumping photocycle to be productive, the deprotonated retinal Schiff base must be able to orient towards the cytoplasmic proton donor Asp96. This requirement is fulfilled by the 13-*cis*, 15-*anti* retinal states, but not by 15-*syn*. The formation of the unproductive 15-*syn* deprotonated retinal state with the Schiff base pointing towards the extracellular side of the membrane is avoided by rendering unlikely the accumulation of 15-*syn* states prior to proton transfer. Relative to the twisted K intermediate, it costs ~16 kcal mol^{-1} less energy for the retinal to escape to a cytoplasmic orientation of the 15-*anti* retinal Schiff base than to proceed to a 15-*syn* state. These observations are consistent with previous experiments that argue in favor of a 15-*anti* retinal conformation during the light-adapted photocycle[69–71] and illustrate the importance of computing and

dissecting the energy profiles associated with proton transfer and retinal configurational changes.

Acknowledgements

This work was financed by the Deutsche Forschungsgemeinschaft (SM 63/7).

References

1 D. Oesterhelt and W. Stoeckenius, Functions of a new photoreceptor membrane, *Proc. Natl. Acad. Sci. U. S. A.*, 1973, **70**, 2853–2857.
2 A. Lewis, J. Spoonhower, R. A. Bogomolni, R. H. Lozier and W. Stoeckenius, Tunable laser resonance Raman spectroscopy of bacteriorhodopsin, *Proc. Natl. Acad. Sci. U. S. A.*, 1974, **71**, 4462–4466.
3 B. Aton, A. G. Doukas, R. H. Callender, B. Becher and T. G. Ebrey, Resonance Raman studies of the purple membrane, *Biochemistry*, 1977, **16**, 2995–2999.
4 K. Bagley, G. Dollinger, L. Eisenstein, A. K. Singh and L. Zimányi, Fourier transform infrared difference spectroscopy of bacteriorhodopsin and its photoproducts, *Proc. Natl. Acad. Sci. U. S. A.*, 1982, **79**, 4972–4976.
5 J. B. Hurley, B. Becher and T. G. Ebrey, More evidence that light isomerizes the chromophore of purple membrane protein, *Nature*, 1978, **272**, 87–88.
6 M. Tsuda, M. Glaccum, B. Nelson and T. G. Ebrey, Light isomerizes the chromophore of bacteriorhodopsin, *Nature*, 1980, **287**, 351–353.
7 R. Neutze, E. Pebay-Peyroula, K. Edman, A. Royant, J. Navarro and E. M. Landau, Bacteriorhodopsin: a high-resolution structural view of vectorial proton transport, *Biochim. Biophys. Acta*, 2002, **1565**, 144–167.
8 J. Herzfeld and J. C. Lansing, Magnetic resonance studies of the bacteriorhodopsin pump cycle, *Annu. Rev. Biophys. Biomol. Struct.*, 2002, **31**, 73–95.
9 T. Hirai and S. Subramaniam, Structural insights into the mechanism of proton pumping by bacteriorhodopsin, *FEBS Lett.*, 2003, **545**, 2–8.
10 H. Luecke and J. K. Lanyi, Structural clues to the mechanism of ion pumping in bacteriorhodopsin, *Adv. Protein Chem.*, 2003, **63**, 111–130.
11 J. K. Lanyi, Bacteriorhodopsin, *Annu. Rev. Physiol.*, 2004, **66**, 665–688.
12 H. J. M. de Groot, G. S. Harbison, J. Herzfeld and R. G. Griffin, Nuclear magnetic resonance study of the Schiff base in bacteriorhodopsin: counterion effects on the ^{15}N shift anisotropy, *Biochemistry*, 1989, **28**, 3346–3353.
13 T. Marti, S. J. Rösselet, H. Otto, M. P. Heyn and H. G. Khorana, The retinylidene Schiff base counterion in bacteriorhodopsin, *J. Biol. Chem.*, 1991, **266**, 18674–18683.
14 R. Needleman, M. Chang, B. Ni, G. Váró, J. Fornés, S. H. White and J. K. Lanyi, Properties of $Asp^{212} \rightarrow Asn$ suggest that Asp^{212} and Asp^{85} both participate in a counterion and proton acceptor complex near the Schiff base, *J. Biol. Chem.*, 1991, **266**, 11478–11484.
15 S. Subramaniam, D. A. Greenhalgh and H. G. Khorana, Aspartic acid 85 in bacteriorhodopsin functions both as proton acceptor and negative counterion to the Schiff base, *J. Biol. Chem.*, 1992, **267**, 25730–25733.
16 H. Belrhali, P. Nollert, A. Royant, C. Menzel, J. P. Rosenbuch, E. M. Landau and E. Pebay-Peyroula, Protein, lipid and water organization in bacteriorhodopsin crystals: a molecular view of the purple membrane at 1.9 Å resolution, *Structure*, 1999, **7**, 909–917.
17 H. Luecke, B. Schobert, H.-T. Richter, J.-P. Cartailler and J. K. Lanyi, Structure of bacteriorhodopsin at 1.55 Å resolution, *J. Mol. Biol.*, 1999, **291**, 899–911.
18 Y. Gat and M. Sheves, A mechanism for controlling the pK_a of the retinal protonated Schiff base in retinal proteins. A study with model compounds, *J. Am. Chem. Soc.*, 1993, **115**, 3772–3773.
19 S. Hayashi and I. Ohmine, Proton transfer in bacteriorhodopsin: Structure, excitation, IR spectra, and potential energy surface analyses by an ab initio QM/MM method, *J. Phys. Chem. B*, 2000, **104**, 10678–10691.
20 B. Schobert, J. Cupp-Vickery, V. Hornak, S. O. Smith and J. K. Lanyi, Crystallographic analysis of the K intermediate of bacteriorhodopsin: Conservation of free energy after photoisomerization of the retinal, *J. Mol. Biol.*, 2002, **321**, 715–726.
21 S. Hayashi, E. Tajkhorshid and K. Schulten, Structural changes during the formation of early intermediates in the bacteriorhodopsin photocycle, *Biophys. J.*, 2002, **83**, 1281–1297.
22 Y. Matsui, K. Sakai, M. Murakami, Y. Shiro, S. Adachi, H. Okumura and T. Kouyama, Specific damage induced by X-ray radiation and structural changes in the primary photoreaction of bacteriorhodopsin, *J. Mol. Biol.*, 2002, **324**, 469–481.
23 S. Hayashi, E. Tajkhorshid, H. Kandori and K. Schulten, Role of hydrogen-bond network in energy storage of bacteriorhodopsin's light-driven proton pump revealed by *ab initio* normal-mode analysis, *J. Am. Chem. Soc.*, 2004, **126**, 10516–10517.
24 H. Kandori, M. Belenky and J. Herzfeld, Vibrational frequency and dipolar orientation of the protonated Schiff base in bacteriorhodopsin before and after photoisomerization, *Biochemistry*, 2002, **41**, 6026–6031.
25 A.-N. Bondar, S. Fischer, S. Suhai and J. C. Smith, Tuning of retinal twisting in bacteriorhodopsin controls the directionality of the early photocycle steps, *J. Phys. Chem. B*, 2005, **109**, 14786–14788.
26 R. R. Birge and T. M. Cooper, Energy storage in the primary step of the photocycle of bacteriorhodopsin, *Biophys. J.*, 1983, **42**, 61–69.
27 K. J. Rothschild, P. Roepe, J. Lugtenburg and J. A. Pardoen, Fourier transform infrared evidence for Schiff base alteration in the first step of the bacteriorhodopsin photocycle, *Biochemistry*, 1984, **23**, 6103–6109.
28 A. Warshel, Conversion of light energy to electrostatic energy in the proton pump of *Halobacterium halobium*, *Photochem. Photobiol.*, 1979, **30**, 285–290.
29 B. Honig, T. Ebrey, R. H. Callender, U. Dinur and M. Ottolenghi, Photoisomerization, energy storage, and charge separation: a model for light energy transduction in visual pigments and bacteriorhodopsin, *Proc. Natl. Acad. Sci. U. S. A.*, 1979, **76**, 2503–2507.
30 O. Kaliski, M. Ottolenghi, B. Honig and R. Korenstein, Environmental effects on formation and photoreaction of the M_{412} photoproduct of bacteriorhodopsin: Implications for the mechanism of proton pumping, *Biochemistry*, 1981, **20**, 649–655.
31 K. Gerwert, G. Souvignier and B. Hess, Simultaneous monitoring of light-induced changes in protein side-group protonation, chromophore isomerization, and backbone motion of bacteriorhodopsin by time-resolved Fourier-transform infrared spectroscopy, *Proc. Natl. Acad. Sci. U. S. A.*, 1990, **87**, 9774–9778.
32 M. S. Braiman, O. Bousché and K. J. Rothschild, Protein dynamics in the bacteriorhodopsin photocycle: Submillisecond Fourier transform infrared spectra of the L, M, and N photointermediates, *Proc. Natl. Acad. Sci. U. S. A.*, 1991, **88**, 2388–2392.
33 K. Edman, A. Royant, G. Larsson, F. Jacobson, T. Taylor, D. van der Spoel, E. M. Landau, E. Pebay-Peyroula and R. Neutze, Deformation of helix C in the low temperature L-intermediate of bacteriorhodopsin, *J. Biol. Chem.*, 2004, **279**, 2147–2158.
34 J. K. Lanyi and B. Schobert, Mechanism of proton transport in bacteriorhodopsin from crystallographic structures of the K, L, M_1, M_2, and M_2' intermediates of the photocycle, *J. Mol. Biol.*, 2003, **328**, 439–450.
35 S. Subramaniam and R. Henderson, Molecular mechanism of vectorial proton translocation by bacteriorhodopsin, *Nature*, 2000, **406**, 653–657.
36 E. Tajkhorshid, J. Baudry, K. Schulten and S. Suhai, Molecular dynamics study of the nature and origin of retinal's twisted structure in bacteriorhodopsin, *Biophys. J.*, 2000, **78**, 683–693.
37 T. Okada, M. Sugihara, A.-N. Bondar, M. Elstner, P. Entel and V. Buss, The retinal conformation and its environment in rhodopsin in light of a new 2.2 Å crystal structure, *J. Mol. Biol.*, 2004, **342**, 571–583.
38 V. Lemaître, P. Yeagle and A. Watts, Molecular dynamics simulations of retinal in rhodopsin: from the dark-adapted state towards lumirhodopsin, *Biochemistry*, 2005, **44**, 12667–12680.
39 A.-N. Bondar, M. Elstner, S. Suhai, J. C. Smith and S. Fischer, Mechanism of primary proton transfer in bacteriorhodopsin, *Structure*, 2004, **12**, 1281–1288.
40 A.-N. Bondar, S. Fischer, J. C. Smith, M. Elstner and S. Suhai, Key role of electrostatic interactions in bacteriorhodopsin proton transfer, *J. Am. Chem. Soc.*, 2004, **126**, 14668–14677.
41 K. Ludman, C. Gergely and G. Váró, Kinetic and thermodynamic study of the bacteriorhodopsin photocycle over a wide pH range, *Biophys. J.*, 1998, **75**, 3110–3119.
42 M. J. Field, P. A. Bash and M. Karplus, A combined quantum mechanical and molecular mechanical potential for molecular dynamics simulations, *J. Comput. Chem.*, 1991, **11**, 700–733.

43 M. Elstner, D. Porezag, G. Jungnickel, J. Elsner, M. Haugk, T. Frauenheim, S. Suhai and G. Seifert, Self-consistent-charge density-functional tight-binding method for simulations of complex materials properties, *Phys. Rev. B*, 1998, **58**, 7260–7268.

44 H. Zhou, E. Tajkhorshid, T. Frauenheim, S. Suhai and M. Elstner, Performance of the AM1, PM3, and SCC-DFTB methods in the study of conjugated Schiff base molecules, *Chem. Phys.*, 2002, **277**, 91–103.

45 Q. Cui, M. Elstner, E. Kaxiras, T. Frauenheim and M. Karplus, A QM/MM implementation of the Self-Consistent Charge Density Functional Tight Binding (SCC-DFTB) method, *J. Phys. Chem. B*, 2001, **105**, 569–585.

46 S. Fischer and M. Karplus, Conjugate peak refinement: an algorithm for finding reaction paths and accurate transition states in systems with many degrees of freedom, *Chem. Phys. Lett.*, 1992, **194**, 252–261.

47 B. R. Brooks, R. E. Bruccoleri, B. D. Olafson, D. J. States, S. Swaminathan and M. Karplus, CHARMM: a program for macromolecular energy minimization and dynamics calculations, *J. Comput. Chem.*, 1983, **4**, 187–217.

48 K. Edman, P. Nollert, A. Royant, H. Belrhali, E. Pebay-Peyroula, J. Hajdu, R. Neutze and E. M. Landau, High-resolution X-ray structure of an early intermediate in the bacteriorhodopsin photocycle, *Nature*, 1999, **401**, 822–826.

49 S. Subramaniam, M. Lindahl, P. Bullough, A. R. Faruqi, J. Tittor, D. Oesterhelt, L. Brown, J. Lanyi and R. Henderson, Protein conformational changes in the bacteriorhodopsin photocycle, *J. Mol. Biol.*, 1999, **287**, 145–161.

50 J. K. Lanyi, Molecular mechanism of ion transport in bacteriorhodopsin: insights from crystallographic, spectroscopic, kinetic, and mutational studies, *J. Phys. Chem. B*, 2000, **104**, 11441–11448.

51 J. K. Lanyi and H. Luecke, Bacteriorhodopsin, *Curr. Opin. Struct. Biol.*, 2001, **11**, 415–419.

52 J. Herzfeld and B. Tounge, NMR probes vectoriality in the proton-motive photocycle of bacteriorhodopsin: evidence for an 'electrostatic steering' mechanism, *Biochim. Biophys. Acta*, 2000, **1460**, 95–105.

53 S. Subramaniam and R. Henderson, Crystallographic studies of protein conformational changes in the bacteriorhodopsin photocycle, *Biochim. Biophys. Acta*, 2000, **1460**, 157–165.

54 A.-N. Bondar, M. Elstner, S. Suhai, S. Fischer and J. C. Smith, Direct proton transfer in a putative L-state intermediate of the bacteriorhodopsin photocycle, *Phase Transitions*, 2005, **78**, 5–9.

55 A. Royant, K. Edman, T. Ursby, E. Pebay-Peyroula, E. M. Landau and R. Neutze, Helix deformation is coupled to vectorial proton transport in the photocycle of bacteriorhodopsin, *Nature*, 2000, **406**, 645–648.

56 H. J. Butt, K. Fendler, E. Bamberg, J. Tittor and D. Oesterhelt, Aspartic acids 96 and 85 play a central role in the function of bacteriorhodopsin as a proton pump, *EMBO J.*, 1989, **8**, 1657–1663.

57 H. Otto, T. Marti, M. Holz, T. Mogi, L. J. Stern, F. Engel, H. G. Khorana and M. P. Heyn, Substitution of amino acids Asp-85, Asp-212, and Arg-82 in bacteriorhodopsin affects the proton release phase of the pump and the p*K* of the Schiff base, *Proc. Natl. Acad. Sci. U. S. A.*, 1990, **87**, 1018–1022.

58 J. K. Lanyi, J. Tittor, G. Váró, G. Krippahl and D. Oesterhelt, Influence of the size and protonation state of acidic residue 85 on the absorption spectrum and photoreaction of the bacteriorhodopsin chromophore, *Biochim. Biophys. Acta*, 1992, **1099**, 102–110.

59 D. A. Greenhalgh, S. Subramaniam, U. Alexiev, H. Otto, M. P. Heyn and H. G. Khorana, Effect of introducing different carboxylate-containing side chains at position 85 on chromophore formation and proton transport in bacteriorhodopsin, *J. Biol. Chem.*, 1992, **267**, 25734–25738.

60 J. Heberle, D. Oesterhelt and N. A. Dencher, Decoupling of photo- and proton cycle in the Asp85 → Glu mutant of bacteriorhodopsin, *EMBO J.*, 1993, **12**, 3721–3727.

61 L. S. Brown, Proton transport mechanism of bacteriorhodopsin as revealed by site-specific mutagenesis and protein sequence variability, *Biochemistry (Moscow)*, 2001, **66**, 1249–1255.

62 S. Scheiner and X. Duan, Effect of intermolecular orientation upon proton transfer within a polarizable medium, *Biophys. J.*, 1991, **60**, 874–883.

63 S. Scheiner and E. A. Hillenbrand, Modification of p*K* values caused by change in H-bond geometry, *Proc. Natl. Acad. Sci. U. S. A.*, 1985, **82**, 2741–2745.

64 L. S. Brown, Y. Gat, M. Sheves, Y. Yamazaki, A. Maeda, R. Needleman and J. K. Lanyi, The retinal Schiff base-counterion complex of bacteriorhodopsin: changed geometry during the photocycle is a cause of proton transfer to aspartate 85, *Biochemistry*, 1994, **33**, 12001–12011.

65 I. Rousso, N. Friedman, M. Sheves and M. Ottolenghi, pK_a of the protonated Schiff base and aspartic 85 in the bacteriorhodopsin binding site is controlled by a specific geometry between the two residues, *Biochemistry*, 1995, **34**, 12059–12065.

66 R. Friedman, E. Nachliel and M. Gutman, Application of classical molecular dynamics for evaluation of proton transfer mechanism on a protein, *Biochim. Biophys. Acta*, 2005, **1710**, 67–77.

67 E. Tajkhorshid, B. Paisz and S. Suhai, Role of isomerization barriers in the pK_a control of the retinal Schiff base: a density functional study, *J. Phys. Chem. B*, 1999, **103**, 4518–4527.

68 A. D. Gruia, A.-N. Bondar, J. C. Smith and S. Fischer, Mechanism of a molecular valve in the halorhodopsin chloride pump, *Structure*, 2005, **13**, 617–627.

69 S. P. A. Fodor, J. B. Ames, R. Gebhard, E. M. M. van der Berg, W. Steoeckenius, J. Lugtenburg and R. A. Mathies, Chromophore structure in bacteriorhodopsin's N intermediate: implications for the proton-pumping mechanism, *Biochemistry*, 1988, **27**, 7097–7101.

70 J. B. Ames, S. P. A. Fodor, R. Gebhard, J. Raap, E. M. M. van der Berg, J. Lugtenburg and R. A. Mathies, Bacteriorhodopsin's M_{412} intermediate contains a 13-*cis*, 14-s-*trans*, 15-*anti*-retinal Schiff base chromophore, *Biochemistry*, 1989, **28**, 3681–3687.

71 M. R. Farrar, K. V. Lakshmi, S. O. Smith, R. S. Brown, J. Raap, J. Lugtenburg, R. G. Griffin and J. Herzfeld, Solid state NMR study of [ε-^{13}C]Lys-bacteriorhodopsin: Schiff base photoisomerization, *Biophys. J.*, 1993, **65**, 310–315.

